HEFAT2008
6th International Conference on Heat Transfer, Fluid Mechanics and Thermodynamics
30 June to 2 July 2008
Pretoria, South Africa
Paper number: KM1

EXPERIMENTAL STUDY AND CFD ANALYSIS ON VORTEX TUBE

Kalal M.* Matas R and Linhart J.
*Author for correspondence
Department of Power System Engineering,
University of West Bohemia,
Plzen, 306 14,
Czech Republic,
E-mail: kalal@kke.zcu.cz

ABSTRACT

In this experimental study of the vortex tube performance has been carried out to investigate the parameters affecting vortex tube operation. Four cases have been studied, in which the influences of the tube length L, the number of entrance nozzles Nz, cold air orifice diameters d_c and inlet pressure under various condition. The effects of these parameters on the hot and cold outlet temperature as function of cold air mass ratio (ε) are discussed and presented. And also the coefficient of performance (COP) of the vortex tube as a refrigerator and as a heat pump has been calculated.

Three Dimension numerical modelling of vortex tube has been evolved through CFD analysis by using the k–ε turbulence model. Axial, radial and tangential components of the velocity together with the temperature and pressure fields within the vortex tube are simulated. Predictions from the present CFD simulations were compared with data obtained from our experiments under the same geometrical and operating conditions.

INTRODUCTION

The vortex tube has been used in industrial applications of cooling and heating processes because of a simple, compact, light and quiet in operation device. Compressed air is ejected tangentially through a generator into the vortex spin chamber. At up to sonic speed this air stream revolves toward the hot end where some escapes through the control valve. The remaining air, still spinning, is forced back through the centre of this outer vortex. The inner stream gives off kinetic energy in the form of heat to the outer stream and exits the vortex tube as cold air., as shown schematically in figure 1. The vortex tube was first discovered by Ranque [1] but was revived and improved in efficiency by Hilsch [2].

A recent review of the existing literature is given in Coccerill [3]. In spite of the present uses and the various studies, no adequate physical explanation is available for the actual transport mechanism. Ahlborn, et al, [4] identified the temperature splitting phenomenon of a Ranque–Hilsch vortex tube in which a stream of gas divides itself into a hot and a cold flow as a natural heat pump mechanism, which is enabled by a secondary circulation. Ahlborn, et al. [5] considered the vortex tube as a refrigeration device which could be analyzed as a classical thermodynamic cycle, replete with significant temperature splitting, refrigerant, and coolant loops, expansion and compression branches, and natural heat exchangers.

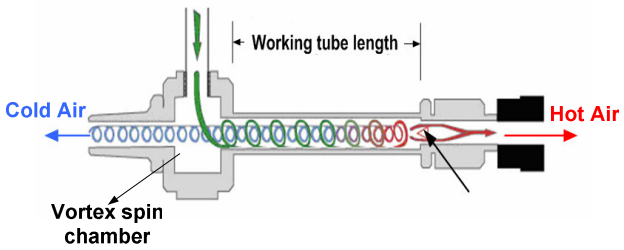

Figure 1 Schematic diagram of the vortex tube.

The effect of various parameters, such as nozzle area, cold orifice area, hot end area and L/D ratio of the tube length to the tube diameter, on the performance of the vortex tube was investigated by Singh [6]. There were experimentally tested variations of the cold air temperature T_c with respect to the change of the hot end area for different L/D. They showed the cold air temperature T_c at all the tested ratios L/D decreased if the hot end was opened. Also the effects of length and diameter on the principal vortex tube are considered by Saidi et al [7]. They showed variation of efficiency versus different L/D of vortex tube. An experimental investigation of the energy separation process in the vortex tube was conducted by Stephan [8]. There were measured temperature profiles at different positions along the vortex tube axis with conclusion the vortex tube length has an important influence on the transport mechanism inside. Ting-Quan [9] they are presented experimental results of the energy separation in the vortex tube under different operating conditions showing the temperature

changes of the cold and hot streams as a function of the inlet pressure. In this study there was found that the hot stream temperature increased with the inlet pressure rising, and that the cold stream temperature decreased with the inlet pressure. Takahama et al [10] they are resulted in several formulas for determining the performance and efficiency of the vortex tubes under a variety of operating conditions, which induced the optimum ratios of the vortex tube dimensions corresponding to the highest efficiency.

NOMENCLATURE

COP	[-]	Coefficient of performance
c_p	[J/kgK]	Specific heat at constant pressure
D_{vt}	[mm]	Inner diameter of vortex tube
d_c	[mm]	Cold end diameter
H	[kJ/kg]	Total enthalpy
k	[W/mK]	Thermal conductivity
L	[mm]	Length of vortex tube
$\dot{m}_c$	[kg/s]]	Mass flow rate of the cold air
$\dot{m}_i$	[kg/s]	Mass flow rate of the hot air
N_z	[-]	Number of entrance nozzle
p	[Pa]	Pressure
$\dot{Q}_c$	[kW]	Cooling power
T	[K]	Temperature
$\vec{u}$	[m/s]	Velocity vector
W_P	[kW]	Work power

Special characters

ΔT	[^{0}C]	Temperature difference
ρ	[kg/m^3]	Density
γ	[-]	Specific heat ratio
τ	[N/m^2]	Stress tensor component
ε	[-]	Cold air mass ratio

Subscripts

c	Cold air
h	Hot air
i	Inlet

So far there are very plenty of available researches to validate the reliability of CFD analyses for investigating the flow and temperature within the vortex tube. Ahlborn et al [11] show the dependence of vortex tube performance on the normalized pressure drop by using a numerical model. Frohlingsdorf and Unger [12] present a detailed analysis of various parameters of the vortex tube through CFD techniques to simulate the phenomenon of flow pattern, thermal separation, pressure gradient etc. And also it utility as a tool for optimal design of vortex tube towards the optimization of number of nozzles, nozzle profiles, cold end diameter, length to diameter ratio, cold and hot gas fractions and comparison of the experimental results with corresponding CFD analysis. Aljwayhel et al. [13] also studied the energy separation mechanism and flow phenomena in a counter flow vortex tube using the CFD code Fluent with the standard k-ε model and the RNG k-ε model. They reported that the RNG k-ε model provides better predictions. This is contrary to results of Skye et al. [14] claimed that for vortex tubes performance, the standard k-ε model performs better than the RNG k-ε model despite using the same commercial CFD code Fluent. Some of these investigators tried to employ higher-order turbulence models but they could not get converged solutions due to numerical instability in solving the strongly swirling flows. The CFD and experimental studies conducted towards the optimization of the Ranque–Hilsch vortex tubes are presented by Upendra et al [15]. They showed the swirl, axial and radial velocity components of the flow, the flow pattern was obtained through CFD. The optimum cold end diameter, the ratios of the vortex tube length to diameter and optimum parameters for obtaining the maximum hot gas temperature and minimum cold gas temperature are obtained through CFD analysis and validated through experiments.

EXPERIMENTAL SETUP

A compressed air with a maximum pressure 800 [kPa] and a maximum volume flow rate of a bout 120 [m3/h], will be used in this study. In this experimental test run, the vortex tube with the inner tube diameter D_{vt} of 21 [mm] and virus tubes length L of 200 up to 1450 [mm] was made of glass. The arrangement of experimental apparatus and measuring devices which is used for the determination of the performance of the counter flow vortex tube is shown in figure2.

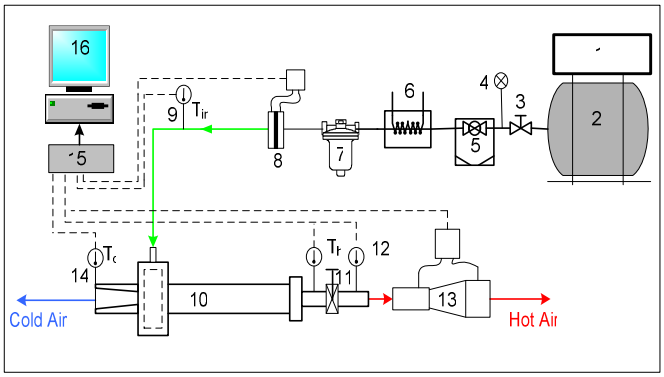

Figure 2 Schematic diagram of the experimental setup

The experimentation was started when the air was compressed by the air compressor (1). The high pressure air passes through the pressure tank (2) to suppress impacts and through the valve (3), where its mass rate is regulated. Inlet pressure is read by the pressure gage (4), and then goes through the dust filter (5) and cooler (6) with cyclone separator (7). The mass flow rate of the inlet air is measured using an orifice (8). Then the compressed air is introduced tangentially into the vortex tube (10), where it expands and separates into the hot and cold air streams. The cold air in the central region leaves the vortex tube near the entrance, while the hot air goes out to the surrounding at the far end of the vortex tube. The control valve (11) controls the flow rate of the hot air. Just after the pipe, the mass flow rate of the hot air is measured using the venture tube (13). Thermocouples numbered 9, 12 and 14 measure the inlet and outlet temperatures. All data about temperatures and pressures are collected with data acquisition system (15) with the output signals being led to the PC (16). The program was written in Lab VIEW 7.2 to control the data logging parameters and to display the obtained results.

Processing of Results

In this section, various experiments on the different components of the vortex tube, setup under various conditions, and four cases have been done to investigate their influence. The influences of the vortex tube length L, the number of entrance nozzles N_z, cold air orifice diameters d_c, have been defined as shown in Table 1.

Case	L [mm]	d_c [mm]	N_z [-]	P_i [bar]	D_{vt} [mm]
1	200, 400, 600, 800, 1000, 1450	12	2	6	21
2	600	8, 10, 12, 14	2	6	21
3	600	10	2, 4	6	21
4	600	10	2	2, 4, 5, 6, 7	21

Table 1 Investigated Case for Various Operation Conditions**.**

In the investigation, the inlet mass flow $\dot{m}_i$ is an important parameter together with ε and the inlet pressure P_{in}, which is controlled by the needle valve placed at hot exhausts. During the experimental test, the vortex tube diameter D_{vt} is always equal to 21 mm. As for the vortex chamber, the inner diameter of the inner ring is always equal to 40 mm. The ε is varied systemically. The ε is defined as follows: $\varepsilon = \dot{m}_c / \dot{m}_i$ where $\dot{m}_c$ represents the mass flow rate of the cold stream released, while $\dot{m}_i$ represents the inlet or total mass flow rate of the pressurized inlet working fluid. Therefore, it changes in the range $0 \leq \varepsilon \geq 1$.

Influence of Tube Length

In order to, investigate the effect of increasing the length of the vortex tube. Six different tube lengths made of glass (200, 400, 600, 800, 1000 and 1450 mm) have been designed and investigated as a function of the ε. The geometry of the system is the one of Case 1 in Table 1. Figure 3(a) and (b) showed hot and cold outlet temperatures and maximum temperature different between hot and cold outlet as a function length tune ratio L/D_{vt} respectively, under the same operation condition. The results for six different tube lengths ratio: 10, 20, 30, 40, 50 and 75, the influence of the tube length is clear from this figure. When the L/D_{vt} increases from 10 up to 40 the hot outlet temperature increases. The cold outlet temperature drop with the L/D_{vt} increases from 10 up to 50. From the analysis result it has been observed that vortex tube can be operated in such a way that it can be used to produce maximum hot air temperature and/or to produce minimum cold air temperature.

Figure 3b shows the maximum ΔT_{hc} increases with increasing the L/D_{vt} from 10 to 50; with longer than that the maximum ΔT_{hc} decreases. Singh [6] concluded that the tube length should be longer than $45D_{vt}$, and also Saidi [7] was suggested the optimum value of L/D_{vt} is within the following ranges $20 \leq L/D_{vt} \leq 55$. In order to, obtain a better performance. In our measurements, the result of the study of the influence of the tube length suggests that a tube length of 1000 mm is good performance, corresponding to L/D_{vt} is about 50. That means there is a critical vortex tube length over which the majority of the energy transfer takes place.

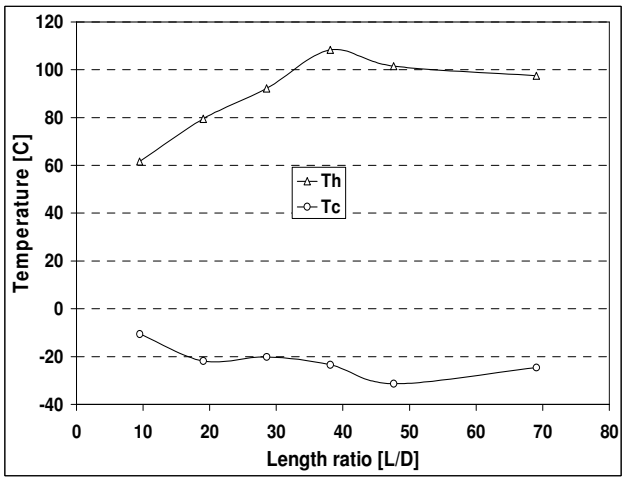

(a)

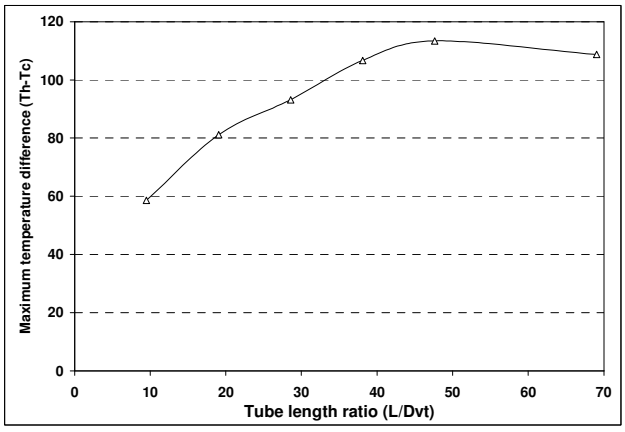

(b)

Figure 3 (a) Hot and cold temperature at deferent length tube ratio (b) Temperature deference at deferent length tube ratio

Influence of the Diameter of Cold Orifice

To determine the effect of the cold air orifice diameter d_c on the hot and cold air temperature, the orifices with different diameters of 8, 10, 12 and 14 mm, were designed, fabricated and obtained experimentally for $L/D_{vt} = 30$ at variations the ε. The geometry of the system is the one of Case 3 in Table 1. The figure 4 shows the outlet air temperature difference as a function of the dimensionless cold air orifice diameter (d_c/D_{vt}). It is shown that for $(d_c/D_{vt}) < 0.57$, increasing (d_c/D_{vt}) causes the outlet air temperature difference to increase and for $(d_c/D_{vt}) > 0.57$, increasing (d_c/D_{vt}) tends the outlet air temperature difference to decrease. From the analysis and experiments it has been observed that vortex tube can be operated in such a way that it can be used to produce maximum hot gas temperature and/or to produce minimum cold gas temperature.

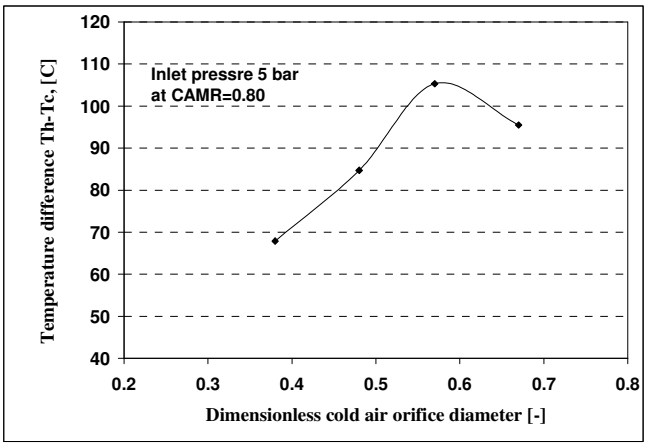

Figure 4 The outlet air temperature difference as function of the dimensionless cold air orifice diameters (L/D_{vt}).

Influence of Entrance Nozzles

To study the effect of number of entrance nozzles, two shapes of nozzle were designed and fabricated, having 2 and 4 entrance, with constant outlet cross-sectional area. Variations of the hot and cold air temperature as function of the ε are shown in Figure 5. With the entrance nozzle number increasing, the flow in the main tube becomes more turbulent due to greater interaction of inlet flows. Therefore the cold and hot streams are mixed in the main tube, leading to energy separation, hot and cold temperature reduction. The result is that with the two entrance nozzles shows better performance than four entrance nozzles.

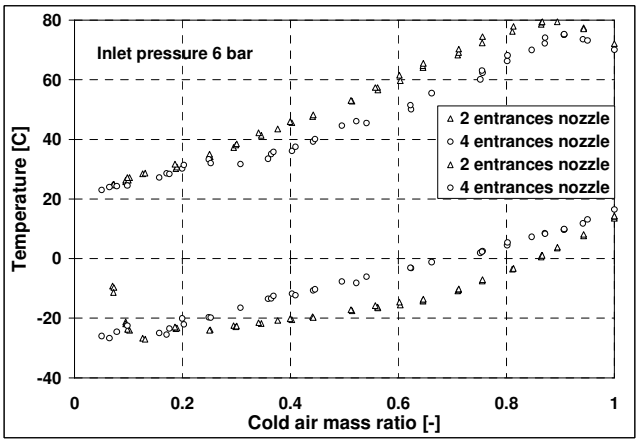

Figure 5 The hot and cold air temperature at different ε and entrances nozzle. Case 3:

Influence of Inlet Pressure

The influence of the inlet pressure at 2, 4, 5, 6 and 7 bar on the temperature of the hot and cold outlet air is clearly distinctive as shown in Figure 6. The geometry of the system is the one of Case 4 in Table 1. Result shows that the temperature of the hot outlet increases with inlet pressure increasing, and that the cold outlet temperature decreases with inlet pressure. The performance of the vortex tube can be improved by increasing the inlet pressure to the critical value. It should be noted that when the inlet pressure increases, with the same system and same cold fraction, the inlet flow increases too.

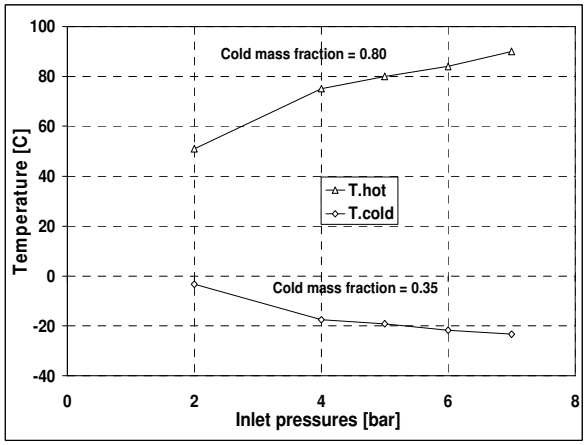

Figure 6 The hot and cold temperature for different inlet pressures, Case 4.

Thermal Efficiencies for Vortex tube

The vortex tube can be used not only as a cooler, but also as a heater. So the definition of the efficiency should consider both effects. For different applications, different efficiencies are used. The coefficient of performance (COP) of a cooler is normally defined as the cooling power Q_c gained by the system divided by the work power W_p input. So the COP of the cooler, denoted by COP_{cr} is expressed as:

$$COP_{cr} = \frac{\dot{Q}_c}{W_p} \tag{1}$$

Here the cooling power can be calculated according to the cooling capacity of the cold exhaust gas (e.g. the heat necessary to heat up the cold exhaust gas from the cold exhaust temperature to the applied temperature. Here T_{in} is chosen.).

$$\dot{Q}_c = \dot{m}_c c_p \left(T_{in} - T_c\right) \tag{2}$$

In a conventional refrigeration system, there is a compressor, so the work power is the input power of the compressor. But in the VT system, usually a compressed gas source is used, so it is not easy to define the work power. By analogy the work used to compress the gas from the exhaust pressure up to the input pressure with a reversible isothermal compression process,

$$W_p = \dot{m}_{in} R_m T_{in} \ln\left(p_{in}/p_a\right) \tag{3}$$

as used in [16], can be expressed as

$$COP_{cr} = \frac{\varepsilon(T_i - T_c)}{\left(\frac{\gamma-1}{\gamma}\right) T_i r_m \ln(p_i/p_a)} \tag{4}$$

For the heat pump, the coefficient of performance is presented as the heating power divided by the work power used. For the vortex tube system, the heating power can be expressed as the heating capacity of the hot exhaust gas.

$$\dot{Q}_h = \dot{m}_h c_p \left(T_h - T_{in}\right) \tag{5}$$

The work power used by the system is taken the same as used above for the cooler. So the coefficient of performance of the vortex tube as a heater, denoted as COP_{hr} is:-

$$COP_{hr} = \frac{\varepsilon(1-\varepsilon)(T_h - T_i)}{\left(\frac{\gamma-1}{\gamma}\right) T_i r_m \ln(p_i / p_a)} \quad (6)$$

Figures 7 and 8 showed the Coefficient of performance of the optimize vortex tube length. There was a substantial increase in the COP.

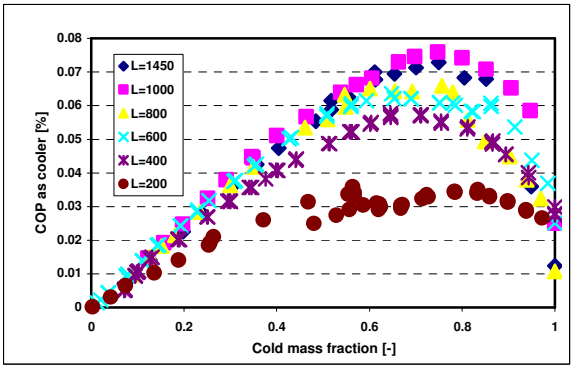

Figure 7 Coefficient of performance of the optimized vortex tube as a refrigerator for difference length.

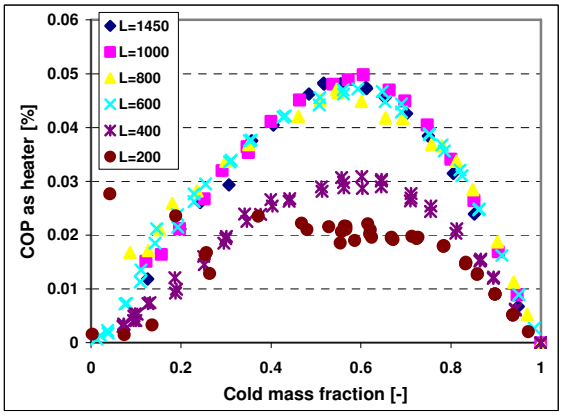

Figure 8 Coefficient of performance of the optimize vortex tube as a heat pump for difference length

The behavior of the COP_{cr} with cold air mass fraction for six different vortex tube length (200, 400, 600, 800, 1000, 1450 mm) at same operating condition to diameter ratio (L/D_{vt}) is depicted in Figure 7. It can be seen that COP_{cr} increases by increasing the length tube up to 1000 mm and it decreases at longer length (1450mm). Also it shows that the maximum COP_{cr} effect occurs as cold air mass fractions between 0.56 and 0.75.

The COP values of the vortex tube for length tube equal 200 to up 1450 mm as a heat machine is shown in figure 8. It is observed that the COP_h of the vortex tube as a heat machine increases with increasing the length of the vortex tube up to 1000 mm and then decreases with longer length.

The COP of vortex tube is very low as compared to COP of Carnot cycle. However this is a unique device which produces both heating and cooling effects simultaneously without using any other form of energy than compressed air at moderate pressure. This device can be used effectively in process environments where heating and cooling outputs of vortex tubes can be concurrently used.

NUMERICAL MODEL

The numerical modelling of a vortex tube has been carried with the CFD system of Fluent. The phenomenon under consideration of the vortex tube is practically an unviscous, steady, compressible and turbulent flow. The equations of mass, momentum and energy conservation per unit mass solved by fluent volume can be expressed as follows:

The Mass Conservation Equation

$$\frac{\partial \rho}{\partial t} + \nabla \cdot (\rho \vec{u}) = 0 \quad (7)$$

The Momentum Conservation Equations

$$\frac{\partial (\rho \vec{u})}{\partial t} + \nabla \cdot (\rho \vec{u}) = -\nabla p + \nabla \cdot \tau \quad (8)$$

Where ρ is the density of the fluid, u is the fluid velocity components, p is the static pressure, τ is the viscous stress tensor, (gravity is neglected).

The Energy Conservation Equation for a fluid region can be written in terms of total enthalpy

$$\frac{\partial (\rho H)}{\partial t} + \nabla \cdot (\rho \vec{u} H) = \frac{\partial p}{\partial t} + \nabla \left(\frac{k}{c_p} \nabla H \right) - \nabla \cdot (\tau \vec{u}) \quad (9)$$

Where H defined as total enthalpy, k and c_p are the thermal conductivity and heat capacity of the fluid, respectively.

CFD Model of Vortex Tube

The model was implemented and meshed using the commercially available geometry pre-processor GAMBIT. The simulations were done with the finite volume code FLUENT. Geometry of the vortex tube simulated by a 3D CFD model is depicted in figure 9. It is shown simple vortex tube with four tangential inlet nozzles. The length is 200mm and inside diameter 21mm.

The geometry comes from the simultaneously measured vortex tube and the hot outlet valve wasn't simulated completely and the control valve was replaced by the pressure outlet with variable value. The only parameter varied during the simulations in this study was the hot air outlet pressure. This results in the variation of mass flow rates in the cold and the hot exit streams.

Boundary Conditions

Computational mesh of the periodical segment has about 1.2 million mixed cells. The pressure and temperature data obtained from the experiments are supplied as input for the analysis. The boundary conditions given to simulate the vortex tube phenomenon at different regions are as follows: The inlet region of the vortex tube (at inlet of nozzle) with inlet mass flow rate 0.035 kg/s was chosen to match our experimental inlet mass flow rate and the total temperature at the inlet was set to

300 K. Pressure boundary condition to the hot end region of vortex tube with pressure varying so as to vary the mass flow at the hot end to obtain the optimum value. And the tube walls were considered to be adiabatic with no slip boundary condition for the velocity components.

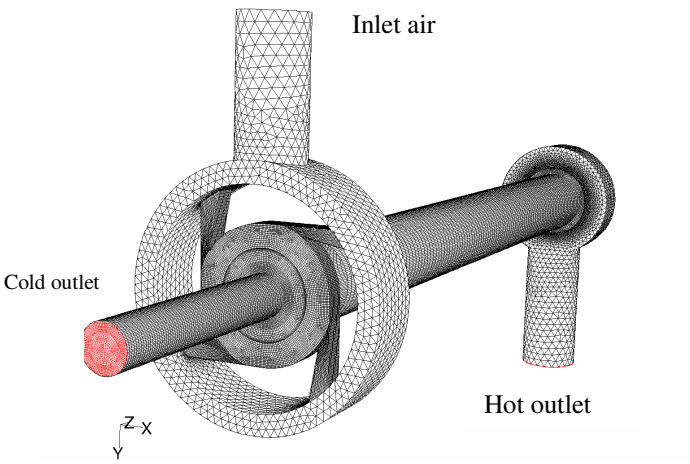

Figure 9. Three dimensional CFD model of vortex tube with four entrance nozzles

PROCESSING OF RESULTS

This section describes a detailed analysis of the CFD model results obtained from FLUENT. The numerical model was seen to agree reasonably with experimental data. However, the primary purpose of the numerical modelling was to develop an understanding of the physical processes that produce the vortex tube's remarkable temperature separation capabilities.

It is clear from Figures 10 that CFD is able to predict a substantial temperature separation for the vortex tube. The total temperature increases in both the radial direction and axial directions.

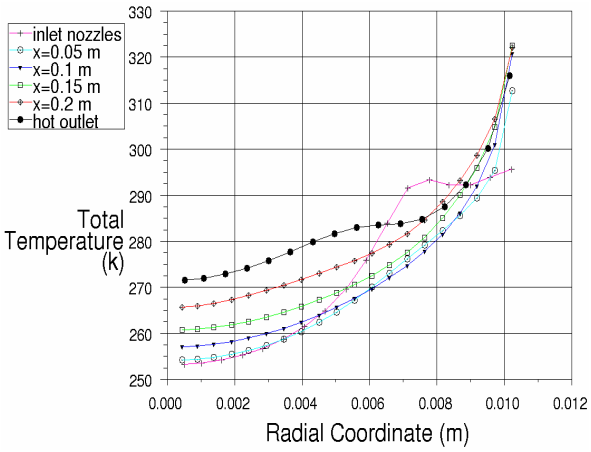

Figure 10 Total temperature as a function of radius at several axial positions.

Figures 11 and 12 illustrate the total pressure and static pressure profiles. It can be seen that both the static and the total pressures are increasing in the radial direction as a result of the centrifugal force that is created by the vortex. However, both static and total pressure decreases as the flow progresses toward the hot outlet near the outer radius in the axial direction. Towards the centre, the flow is in the opposite direction and therefore the pressure increases in the axial direction, albeit a very small amount.

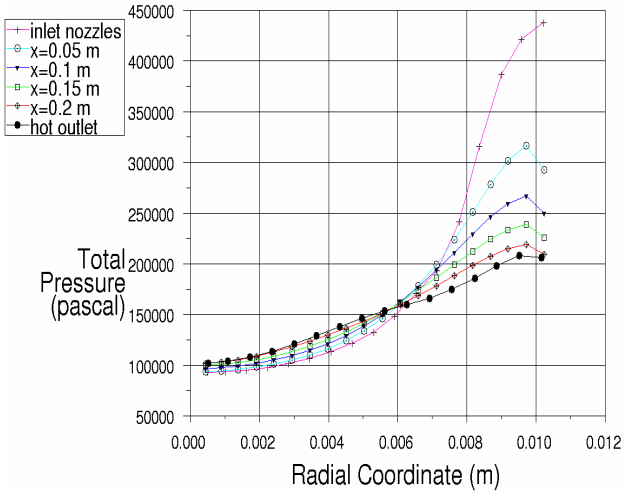

Figure 11 Total pressure as a function of radius at several axial positions.

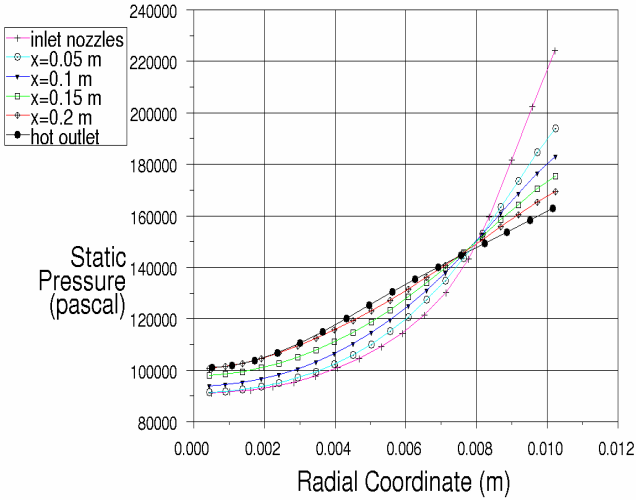

Figure 12 Static pressure as a function of radius at several axial positions.

Figure 13 shows the radial profiles of the axial velocity at different axial locations (x = 50 mm, x = 100 mm, x = 150 mm and x = 200 mm). The maximum axial velocity is near the tube wall and the direction of the flow near the wall is towards the hot end exit and the direction of the flow along the axis is towards the cold end exit. It was observed that the maximum value of the axial velocity decreased with increasing axial distance except at inlet nozzles and at the hot outlet. At axial locations of 50, 100, 150, and 200 mm the maximum axial velocity was found to be 90, 86, 80 and 78 m/s, respectively.

The axial velocity profiles show that the flow reversal takes place at about 6 mm from the centre of the tube. The axial velocity in the cold core is directed towards the cold end exit. The axial velocity in the cold core was found to increase with a decrease in the axial distance.

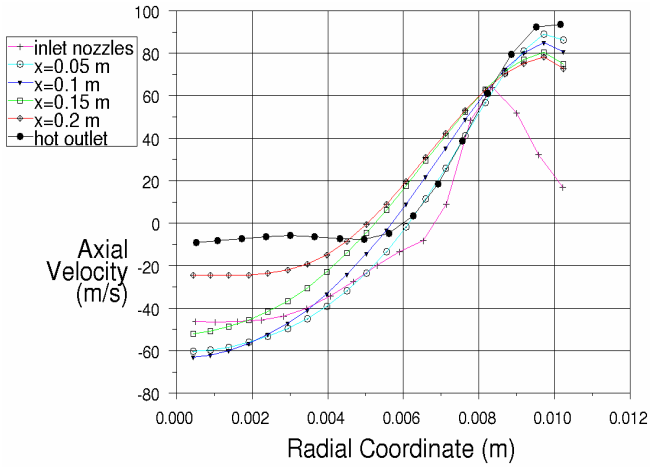

Figure 13 Axial velocities as a function of radius at several axial positions.

Tangential velocity as a function of radius at several axial positions is shown in figure 14. The tangential velocity is negative to all radial direction. The tangential velocity increase in the axial direction and in the radial direction and then begins to decreases at a radius of 5 mm, which is approximately the centre line of the re-circulating region.

Figure 15 shows the radial velocity as a function of radius at several axial positions. As it is shown**,** the magnitude of the radial velocity everywhere is less than 2 m/s except for inlet nozzle and hot outlet; it was found 25 and 7 mm, respectively for short distance at a radius of 6 mm.

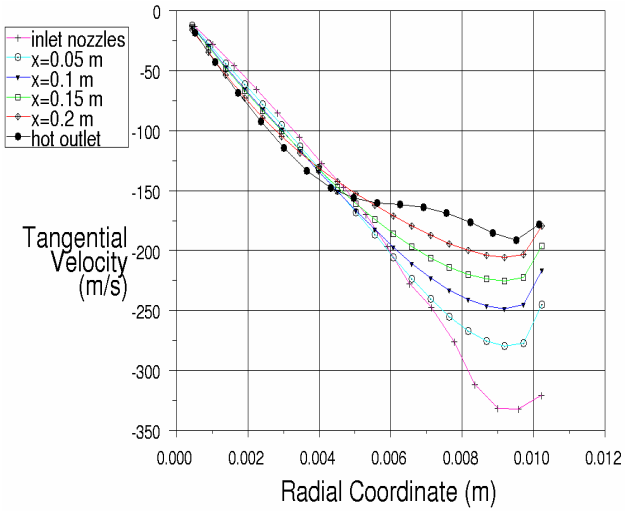

Figure 14 tangential velocities as a function of radius at several axial positions**.**

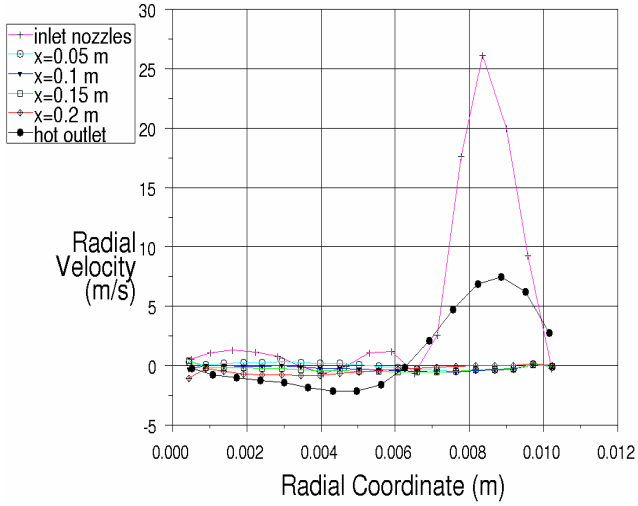

Figure 15 Radial velocities as a function of radius at several axial positions.

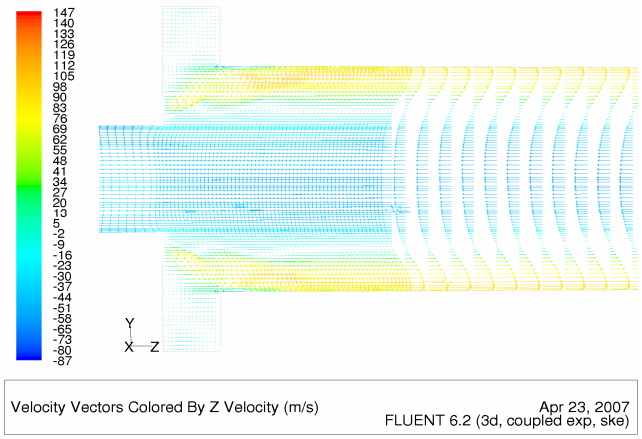

(a)

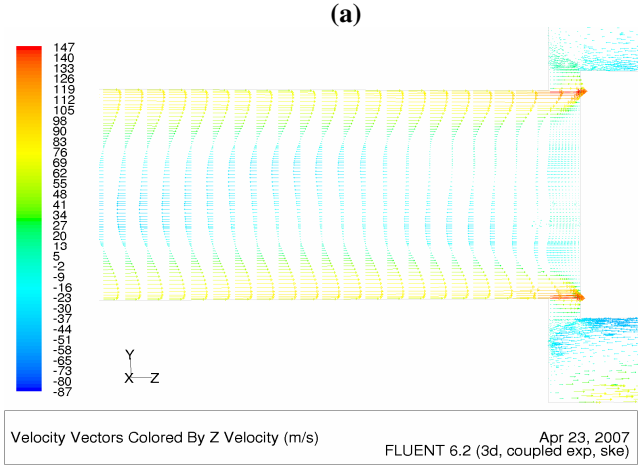

(b)

Figure 16. Velocity vector plot from CFD of cross plane at, (a) inlet and cold outlet (b) hot outlet.

The visualization of the velocity vector profile inside the vortex tube helped to understand the details of fluid flow. The following two figures 16(a) and (b) illustrate the distribution of velocity vector profile at cross plane of inlet, cold air outlet and

hot air outlet, respectively. It can be found that the velocities higher at near the wall than that one in the center. The maximum velocity is about 120m/s at near wall.

COMPARISON OF CFD MODEL AND EXPERIMANTAL DATA

The inlet mass flow rate in the CFD model was specified as a constant 0.0334 kg/s, which is consistent with the measured total temperature at the inlet to the vortex tube for length 200 mm. The results of the experimental model were compared with 3D model. Figures 17 showed the experiments and CFD analysis of the hot and cold outlet temperature of air as a function of the parameter ε.

It can be seen that for 200mm the maximum hot outlet temperature of 49.7 ^{o}C (at ε = 0.56) is obtained from CFD analysis and about 55.5 ^{o}C is obtained from experiments at the same of ε. And a minimum cold outlet temperature of -13.4 ^{o}C (at ε = 0.139) is obtained from CFD analysis and about -17.5 ^{o}C (at ε = 0.073) is obtained from experiments.

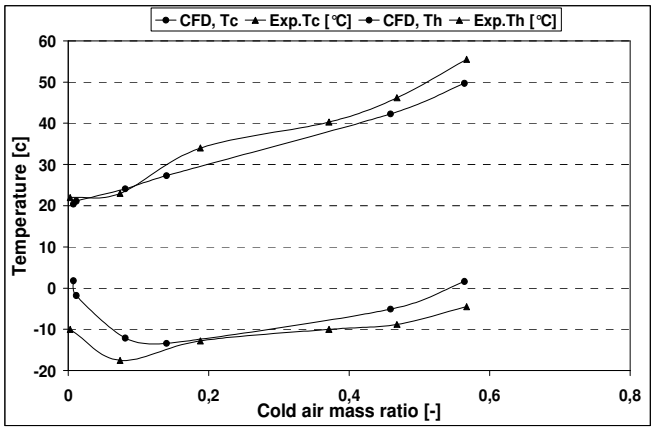

Figure 17 The experiment and CFD analysis of the hot and cold air outlet temperature as a function of CAMR.

CONCLUSION

The experiments were performed in tubes with inner diameter of 21 mm, made of glass. The following constructional parameters were tested and tried to be optimized. Five different vortex tubes of lengths 200, 400, 600, 800, 1000 and 1450 mm, with 2 and 4 entrance nozzles and four different diameters of the cold outlet, namely 8, 10, 12 and 14 mm were tested.

Experimental results of the hot and cold air outlet temperatures of the vortex tube, with the dimensionless cold air mass ratio ε and the inlet air pressure as parameters are presented. It is clear from our experiments that the higher inlet pressure causes the greater temperature difference of the two outlet air streams. And also the analysis shows temperature difference between hot and cold air outlet can be maximized by increasing the length to diameter ratio of vortex tube.

The experimental studies have shown that for 1000 mm length vortex tube, the cold outlet diameter of 12 mm is ideal for the maximum temperature difference between hot and cold air temperature. The investigations have shown that L/D_{vt} = 50 is optimum for achieving best thermal performance for 21 mm diameter vortex tube with 2 entrance nozzles.

The purpose of this study was to create a CFD model of the vortex tube for use as a design tool in optimizing vortex tube performance. The CFD model is 3D steady one numerical modeling of vortex tube has been evolved by using the k–ε turbulence model. Axial, radial and tangential components of the velocity together with the temperature and the pressure fields within the vortex tube are simulated. Predictions from the present CFD simulations were compared with data obtained from our experiments under the same geometrical and operating conditions.

REFERENCES

[1] Ranque GJ. [1933], Experiences sure la detente giratoire avec productions simultaneesd'un echappement d'air chand et d'un echappement d'air froid, J Phys Radium, Vol.4, pp. 112–4.

[2] Hilsch R.[1947], The use of the expansion of gases in a centrifugal field as a cooling process, Rev Sci Instrum, Vol. 8, pp. 108–13.

[3] Coccerill T.[1998], Thermodynamics and Fluid Mechanics of a Ranque–Hilsch Vortex Tube, Ph. D. Thesis, University of Cambridge.

[4] Ahlborn B, Keller JU, Rebhan E. [1988], The Heat Pump in a Vortex Tube, Journal Non-Equilib Thermodyn, Vol. 23 No.2, pp 159–65.

[5] Ahlborn BK, Gordon JM. [2000], The Vortex Tube as a Classical Thermodynamic Refrigeration Cycle, Journal Applied Phys, Vol. 88, No.6, pp 3645–53.

[6] P.K. Singh, R.G.Tathgir, D. Gangacharyulu, and G.S. Grewal. [2004], An experimental performance evaluation of vortex tube, Journal of Institution of Engineers, Vol. 84, pp 149–153.

[7] Saidi M H and Valipour M S. [2003], Experimental modelling of vortex tube refrigerator. Applied thermal engineering. Vol. 23, No. 15, pp 1971-1980.

[8] Stephan K, Lin S, Durst M, Hunag F and Seher D.[1983], An investigation of Energy Separation in a Vortex Tube, International Journal of Heat and Mass Transfer, Vol. 26, No.3, pp 341-388.

[9] Ting-Quan MA, Qing-Guo, Jian YU, Fang YE, and Chong-Fang, 2002. Experimental investigation on energy separation by vortex tubes. 12th international Heat Transfer Conference, 10, Paris.

[10] H. Takahama, and H. Yokosawa. [1981], Energy Separation in Vortex Tubes with a Divergent Chamber, ASME Journal of Heat Transfer, Vol. 103, pp 196-203.

[11] B. Ahlborn, J.U. Keller, R. Staudt, G. Treitz, R. Rebhan. [1994], Limits of Temperature Separation in a Vortex Tube, J Phys D: Appl Phys Vol. 27, pp 480–488.

[12]W. Frohlingsdorf and H. Unger. [1999], Numerical Investigations of the Compressible Flow and the Energy Separation in Ranque–Hilsch Vortex Tube, International Journal Heat Mass Transfer, Vol. 42, pp 415–422.

[13] N.F. Aljuwayhel, G.F. Nellis, S.A. Klein. [2005], Parametric and Internal Study of the Vortex Tube using a CFD model, International Journal Refrigeration, Vol. 28 (3), pp 442–450.

[14] H.M. Skye, G.F. Nellis, S.A. Klein. [2006], Computasion of CFD analysis to empirical data in commercial vortex tube, International Journal Refrigeration Vol. 29, pp 71-80.

[15] Upendra Behera, P.J. Paul, S. Kasthurirengan, R. Karunanithi, S.N. Ram, K. Dinesh and S. Jacob. [2005], CFD analysis and experimental investigations towards optimizing the parameters of Ranque–Hilsch vortex tube, International Journal of Heat and Mass Transfer, Vol. 48, Issue 10, pp 1961-1973.

[16] C.D. Fulton. Ranque`s tube. [1950], J. ASRE Refrigerating Engng, 58: 473-479.